ACS OMEGA

Article

Cite This: ACS Omega 2018, 3, 12412−12421

http://pubs.acs.org/journal/acsodf

Biodegradable Composites Developed from PBAT/PLA Binary Blends and Silk Powder: Compatibilization and Performance Evaluation

Daichi Nakayama,[†,§] Feng Wu,[†,‡] Amar K. Mohanty,[†,‡] Shinji Hirai,[*,§] and Manjusri Misra[*,†,‡]

[†]Bioproduct Discovery and Development Centre, Department of Plant Agriculture, University of Guelph, Crop Science Building, Guelph, ON N1G 2W1 Ontario, Canada

[‡]School of Engineering, University of Guelph, Thornbrough Building, Guelph, ON N1G 2W1 Ontario, Canada

[§]Division of Production Systems Engineering, Muroran Institute of Technology, 27-1 Mizumoto-cho, Muroran, Hokkaido 050-8585, Japan

ABSTRACT: Silk fibroin powder and biodegradable polybutylene adipate terephthalate (PBAT)/poly lactide (PLA) blends were melt-mixed together to fabricate natural and synthetic polymers as possible new sources of biomaterials. Morphological observations conducted through scanning electron microscopy indicated poor dispersion of the silk powder agglomerates, which resulted from strong hydrogen interactions between silk powder chains in the PBAT/PLA matrix. Although the silk powder agglomerates decreased the mechanical properties, as silk powder fractions increased, the ternary blend with 10 wt % silk powder still displayed high impact strength of 108 J/m and tensile modulus of 1.2 GPa. On the basis of mechanical analysis, this blend offered potential applications in fields which required high impact strength. Blends which contained Joncryl experienced a decrease in storage modulus. Furthermore, rheological studies confirmed that the viscosity of the PBAT/PLA/Silk powder blends decreased, which indicated possible weakening of hydrogen bonds between the silk chains, caused by the reaction between the epoxy groups of Joncryl. This reaction provides a possible method to improve the processability of this natural polymer and to improve its distribution in polymer blends.

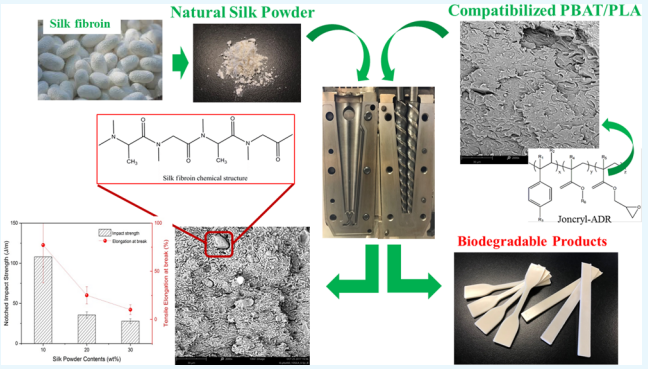

INTRODUCTION

Biodegradable polymeric materials have shown promising potential to replace traditional petro-based plastics in various applications because of environmental and sustainability concerns. Currently, the most widely used polymers are synthetic polymers because of their superior performance such as good mechanical properties, thermal stability, and processability, either for commonplace plastics or biomedical applications.[1] In the past, research has been done on creating synthetic-based, biodegradable polymers such as poly(butylene succinate), but with technology advances, research has begun to bridge the gap between synthetic biodegradable polymers and biobased biodegradable polymers.

In recent decades, other important kinds of biodegradable materials called natural polymers have peaked the interest of researchers. Natural polymers were used as consumptive materials because they were naturally sourced, totally biocompatible, and exhibited good mechanical properties such as high modulus and strength.[2] Compared to synthetic polymers, natural polymers usually possessed poor thermal stability because of their low decomposition temperature and poor melting flowability because of the strong intramolecular interactions (such as hydrogen bonding). Pretreatment is usually performed on natural polymers, even though it is typically a rather high-cost process. To solve the problems previously mentioned, there are various methods being investigated to take advantage of the processability of synthetic polymers. These methods include solution or melt blending natural polymers with synthetic biodegradable polymers directly.

The successful preparation of vinyl-alcohol copolymers/starch blends and their commercial application known as Mater-Bi are good examples of blending modifications.[3] Besides starch, other natural polymers such as collagen, chitosan, silk, elastin, and cellulose have also been developed and researched for different kinds of applications.[2] Silkworm silk has been used in textile applications for thousands of years, and now, silk fibroin macromolecules have been used in the form of films,[4] hydrogels,[5] foams,[6] coating materials,[7] and powders.[8,9] These materials have been extensively studied as a possible source of

Received: April 26, 2018
Accepted: July 25, 2018
Published: October 1, 2018

DOI: 10.1021/acsomega.8b00823
ACS Omega 2018, 3, 12412−12421

Table 1. Mechanical Properties of the PBAT/PLA/Silk Powder Blends with and without Joncryl

matrix	Joncryl (phr)	tensile modulus (MPa)	tensile strength (MPa)	elongation at yield (%)	elongation at break (%)	flexural modulus (MPa)	flexural strength (MPa)	impact strength (J/m)
PLA	0	3637 ± 327	78.8 ± 1.8	2.76 ± 0.19	3.73 ± 0.76	3684 ± 240	115 ± 4.3	15 ± 1.5
PBAT	0	73 ± 2	26.3 ± 0.6	343 ± 5.0	357 ± 18	99 ± 0.78	4.67 ± 0.03	nonbreak
PBAT 60/PLA40	0	1320 ± 70	31.9 ± 0.9	3.07 ± 0.16	183 ± 12	1250 ± 16.2	38.5 ± 0.5	474 ± 34
	0.3	1630 ± 52	34.5 ± 0.7	3.06 ± 0.05	142 ± 7	1409 ± 23.3	42.2 ± 0.7	522 ± 12
	0.5	1647 ± 92	33.5 ± 0.5	3.02 ± 0.04	149 ± 9	1375 ± 5.8	40.9 ± 0.3	535 ± 49
10% Silk powder	0	1120 ± 120	24.1 ± 0.5	3.97 ± 0.43	77.2 ± 39.2	1200 ± 6.2	35.5 ± 0.2	108 ± 12
	0.3	1490 ± 73	26.8 ± 0.5	3.20 ± 0.02	47.9 ± 12.9	1312 ± 15.4	37.8 ± 0.6	71 ± 8
	0.5	1347 ± 89	25.7 ± 0.4	3.54 ± 0.14	49.5 ± 13.0	1261 ± 17.7	37.1 ± 0.6	88 ± 20
20% Silk powder	0	1262 ± 30	22.8 ± 0.5	3.41 ± 0.14	25.1 ± 9.0	1265 ± 21.8	33.6 ± 0.6	36 ± 4
30% Silk powder	0	1224 ± 99	20.4 ± 0.6	3.31 ± 0.15	10.1 ± 5.1	1285 ± 39.5	31.6 ± 1.4	28 ± 3

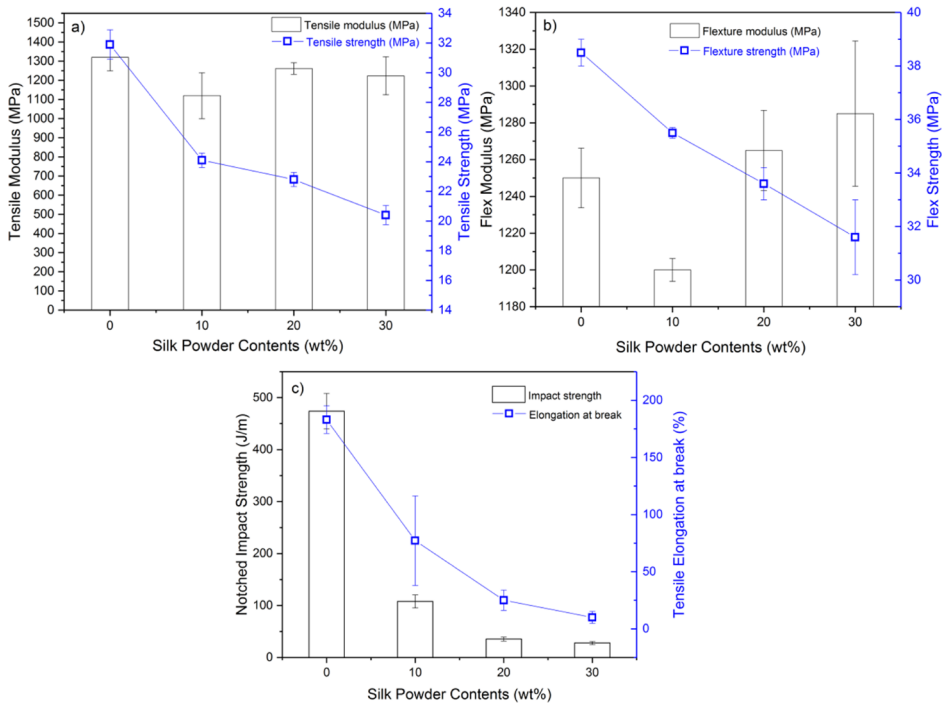

Figure 1. Mechanical properties of PBAT/PLA/silk powder blends as a function of silk content: (a) tensile modulus and strength; (b) flexural modulus and strength; and (c) notched Izod impact strength and tensile elongation at break.

biomaterials for nontextile applications, demonstrating a potential application in the preparation of biocomposites.[4] The literature reported that the three-point bending strength and modulus for the heat compression silk resins were found to be 80 MPa and 5.0 GPa, respectively, which were much higher than those of epoxy and polylactide (PLA).[10] Therefore, silk fibroin was also blended with other polymers such as nylon 6,[11] polyvinyl alcohol,[12] polyurethane,[13] and poly(acrylic acid)[14] to study the interactions between silk and synthesized polymers. It was expected that these synthetic polymers would possess improved mechanical properties. The main disadvantage of these blends was that solutions such as LiBr aqueous were required because common soluble forms of silk are not easily obtained.[2] Compared to solution blending, melt blending is more environmentally friendly and cost effective. However, there is very little research carried out in regards to the use of these new materials and melt blends of silk with other polymers because of the poor compatibility and difficulty in dispersion of the natural polymers.[15] In this study, we blended silk powder with synthesized biopolymers by an economic melt extrusion method and then explored the compatibility and performance of these two different biodegradable polymers to address the possible application of these natural biopolymers.

Natural polymers are studied extensively in the biomedical fields such as tissue engineering,[16] wound healing,[17] and drug delivery.[18] Because of the good mechanical, chemical, and biological properties of natural polymers, blending them with synthesized biodegradable polymers can broaden their applications in customary fields such as food packaging[19] and commercial films.[20] Two important biodegradable polymers, PLA and polybutylene adipate terephthalate (PBAT), were chosen as the matrix material to blend with silk powder. As one of the biodegradable polymers, PLA has been widely studied as a sustainable alternative to petro-based products in commodity applications because of its high mechanical strength and renewable resource polymerization. However, neat PLA exhibits inherent brittleness with poor impact and tear resistance.[21] PBAT, a biodegradable aliphatic−aromatic copolyester, exhibits super-tough properties and a nonbreak notched impact behavior but has a very low tensile modulus.[22] PBAT can be used for toughening and improving elongation-at-break of other biopolymers.[23] Therefore, PBAT/PLA blends were chosen in

DOI: 10.1021/acsomega.8b00823
ACS Omega 2018, 3, 12412−12421

our study to prepare a matrix with balanced stiffness−toughness properties.

Former research regarding the properties of newly developed blends of natural and synthetic polymers showed that the compatibility between the silk and synthesized polymers was rather poor.[15] In the present study, water-soluble superfine silk powder with mean size of ∼7 μm was originally blended with commercially available PBAT/PLA to prepare ternary blends by a melt extrusion process. The objective of this paper was to identify the melt processability of natural biopolymers made with silk powder and to evaluate the processability and compatibility when blended with the synthesized biopolymers. Furthermore, this paper intended to expand the potential applications of these biopolymers by economic melt blending method to solve the environmental concerns caused by the petro-based plastics. The compatibility and mechanical properties were analyzed to address the key problems and possible modifications in the preparation of these blends to obtain a high performance. Investigation on the morphology and compatibility with and without a commercial compatibilizer, Joncryl ADR-4368, was carried out to evaluate the structure−property relationship of the natural/synthesized polymer blends, targeted to improve the processability and dispersion within this natural biopolymer.

RESULTS AND DISCUSSION

Mechanical Properties and Morphology Observation.

The PBAT60/PLA40 binary blends were prepared in our research as a masterbatch because of their balanced stiffness−toughness properties. The binary blends show a tensile modulus of ∼1.3 GPa, elongation at break of ∼190%, and high notched impact strength of ∼480 J/m without any compatibilizer (Table 1).

The influence of the silk powder contents on the mechanical properties of the blends is demonstrated in Figure 1. Except for the almost unchanged tensile modulus, both the tensile and flexure strengths decreased greatly with the increase of silk powder, as shown in Figure 1. The decreased strength is attributed to the absence of shear yielding during stretching. The elongation at break also decreased dramatically, from ∼180 to ∼10% when 30 wt % silk powders were added. According to former research, compressed silk powder samples showed a high flexural modulus of 4500 MPa,[10] where the flexural modulus increased slightly in the presence of 20 and 30 wt % silk powders. However, the flexural modulus of 10 wt % silk powder composites was lower compared to the blending matrix because the enhancing effect of silk powder was compromised by the poor compatibility between the matrix and silk powder at lower silk powder content. Although the matrix (PBAT60/PLA40) shows high notched impact strength of ∼480 J/m, the impact strength of the blends decreased to ∼100 J/m even in the presence of only 10 wt % silk powder, as shown in Figure 1c. The decreased impact strength is the result of poor compatibility between the matrix and silk powder phases. The existing silk powder agglomerates in the matrix were believed to be the cause of weakness in the materials because no linkage existed in the interface. To check the dispersion of the silk powder in the blends, the silk powder before processing and surfaces of the impact-fractured processed blends are observed by scanning electron microscopy (SEM) and shown in Figures 2 and 3, respectively.

It was observed from the SEM images that the large silk powder agglomerates were dispersed in the PBAT/PLA matrix,

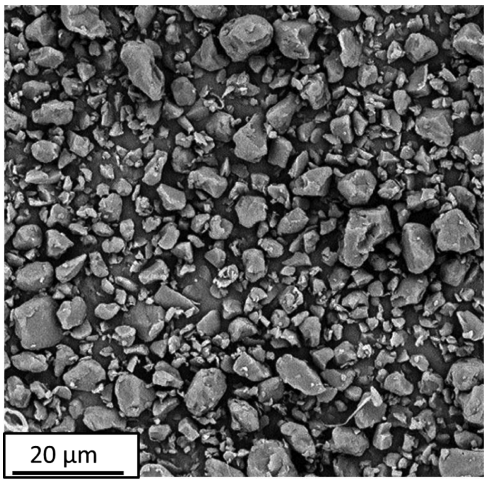

Figure 2. Morphology of the silk powder observed by SEM (magnification 3000×).

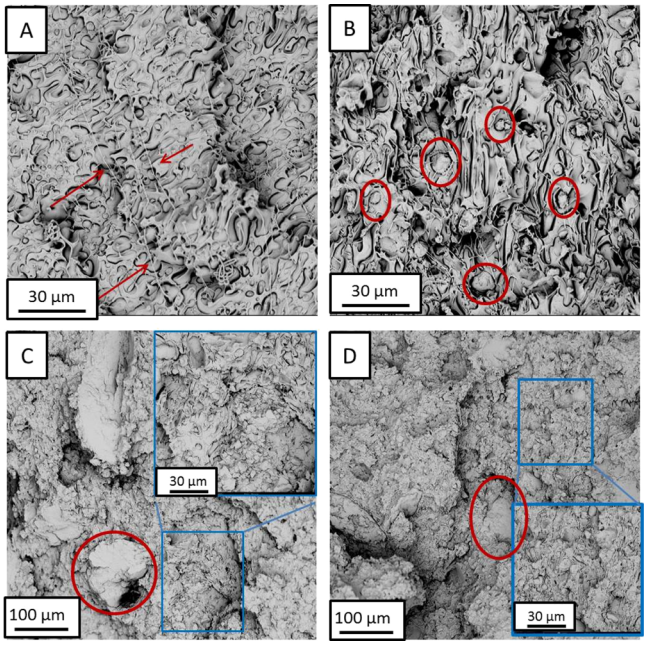

Figure 3. SEM observations of the noncompatibilized silk powder/polyester blends with different silk powder loadings (impact fracture surface): (A) PBAT/A40; (B) PBAT/A40/10Silk; (C) PBAT/A40/20Silk; and (D) PBAT/A40/30Silk. The red arrow indicates the fibrils, whereas the red circle indicates the silk powder agglomerates.

as marked by red circles in Figure 3. The gap between the PBAT/PLA matrix and silk powder was clearly observed, indicating the poor compatibility between the two different polymers (synthesized polymer PBAT/PLA and natural polymer silk powder). As shown in Figure 3, PBAT60/PLA40 formed a cocontinuous structure because of the close composition ratios.[24] Additionally, the formation of large amounts of fibrils (as indicated by the red arrow in Figure 3a) resulted from the fracture of super-tough PBAT under impact. This greatly contributed to the high impact strength of the masterbatch. The formation of the fibrils in PBAT/PLA blends was also observed in the research conducted by Farsetti.[25] With the addition of 10 wt % silk powder, the sample still displayed a tough break, although the amounts of fibrils decreased compared to that of the PBAT/A40 matrix. The notched

DOI: 10.1021/acsomega.8b00823
ACS Omega 2018, 3, 12412−12421

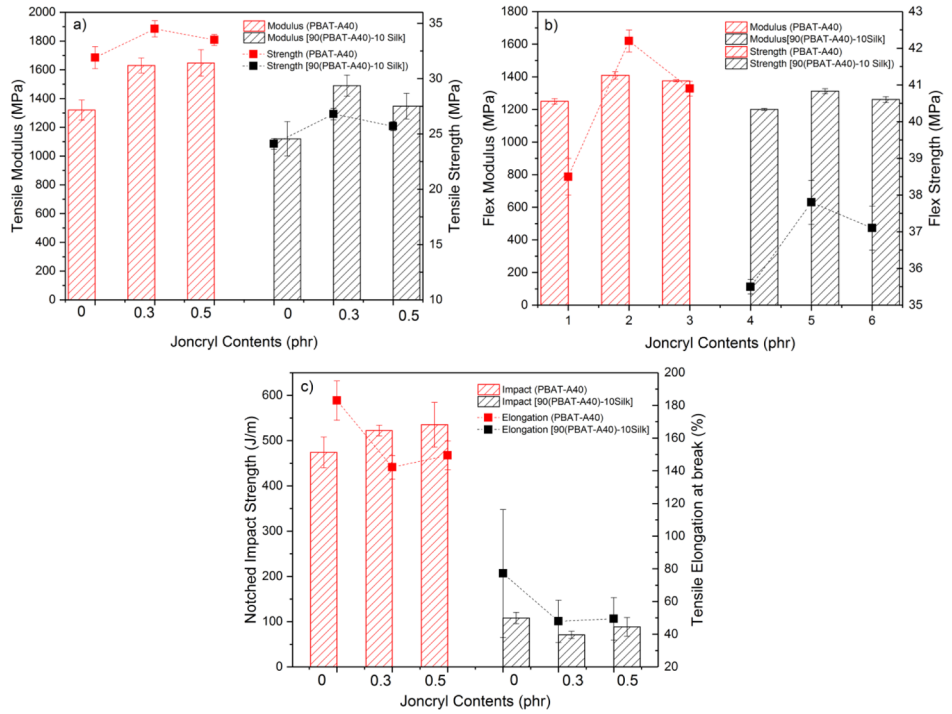

Figure 4. Effect of Joncryl on the mechanical properties of the PBAT/PLA/silk powder blends: (a) tensile modulus and strength; (b) flexural modulus and strength; and (c) the notched Izod impact strength and tensile elongation at break.

impact strength of the blends remained ∼100 J/m because the size of the dispersed silk powder particles was much smaller compared to the other two samples with high silk powder loadings and the formation of some fibrils enhanced impact strength. The samples changed from tough to brittle fractures at 20 wt % silk powder, which can be seen from the SEM photos shown in Figure 3c. Compared to the uniform dispersed pure silk powder with size of ∼7 μm, shown in Figure 2, the size of the large silk powder agglomerate was around 100 μm, indicating the serious agglomeration of the fillers because of the high hydrophilic properties. The fracture surface was smooth, and the fibrils which resulted from the break of PBAT also disappear because of the existing large silk powder particulates (seen from the enlarged photos in Figure 3c,d). The smooth break surface cannot consume energy during fracture, leading to the poor impact strength of ∼35 J/m at 20 wt % silk powder, with only 7% of the PBAT/PLA matrix.

Because the poor compatibility between the silk powder and PBAT/PLA matrix suppressed the mechanical properties of the matrix dramatically, we introduced a commercial chain extender, Joncryl ADR-4368, to research the compatibilizer effect on PBAT/PLA and silk powder. Joncryl has proven to be a good compatibilizer for PLA and PBAT in the former research.[26−28] The effect of Joncryl on the mechanical properties of the PBAT/PLA binary matrix and 90 wt % matrix with 10 wt % silk powder ternary blends was researched and the resulting mechanical properties are shown in Figure 4.

The mechanical properties tested show that the introduction of 0.3 phr Joncryl increased the mechanical properties of the PBAT/PLA matrix, except for the elongation at break. The notched impact strength increased with the increasing amounts of Joncryl, likely due to the esterification reaction that occurred between the polyester hydroxyl/carboxyl functional groups with the epoxy group in Joncryl. This finding has been confirmed in our group's former research.[28] The newly formed copolymer could have increased the compatibility between PBAT and PLA, which may have led to the increased impact strength which required strong interfacial interactions in the blends. Conversely, the elongation at break decreased with the increase of Joncryl. The difference is a result of different break modes under impact (rapid) and stretch (slow) break. Super strong adhesion at the interface was necessary for the high impact, whereas the high adhesion was not beneficial for debonding and matrix yielding, which was required for the high elongation behavior.[29] Less debonding and matrix yielding would also influence the yield strength during stretching, leading to the lower yield strength at 0.5 phr Joncryl, as shown in Figure 4a.

The resulting mechanical properties of ternary blends in Figure 4 show that the modulus and strength (tensile and flexural) reach the highest values at 0.3 phr Joncryl and then decreased at 0.5 phr Joncryl. This was similar to that of the PBAT/PLA binary matrix. This means that Joncryl mainly worked on improving the PBAT/PLA interface rather than the silk powder and PBAT/PLA interface. Our research also indicated that the impact strength and tensile elongation at break both decreased even when Joncryl was introduced into the blends, regardless of the amount added. The interface between the silk powder and PBAT/PLA was improved minimally. The smooth and large-sized silk powder agglomerates served as the weaknesses during the break of the material, which led to the lower impact strength and elongation at break. This is clearly revealed by the morphology observation in SEM images, shown in Figure 5.

Compared to that of the PBAT/PLA without Joncryl shown in Figure 3, the interface between PBAT and PLA was greatly improved with the additional of Joncryl. The gap between PLA and PBAT becomes an issue as the size of the dispersed PLA decreases. The gap and decreased dispersed size of the PLA benefit the macroproperties of the materials by increasing stiffness and toughness. For the ternary blends, although Joncryl

DOI: 10.1021/acsomega.8b00823
ACS Omega 2018, 3, 12412−12421

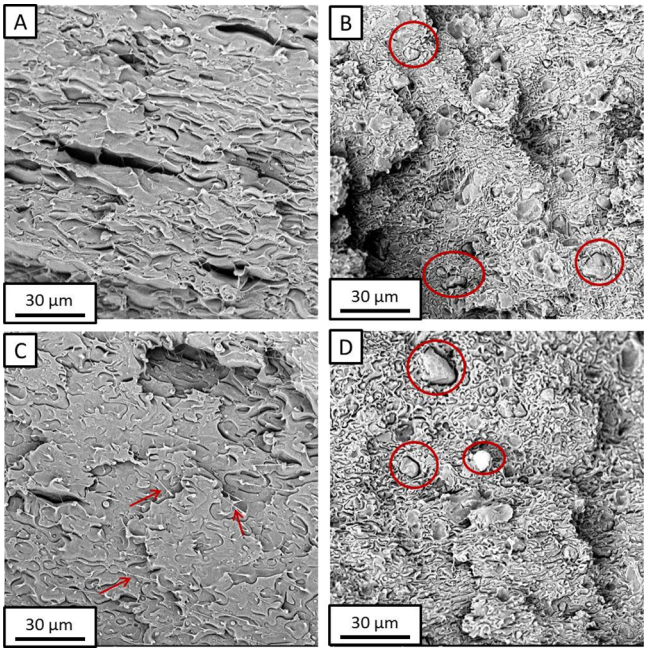

Figure 5. SEM observation of the compatibilized silk powder/polyester blends with 0.5 phr Joncryl (impact fracture surface): (A) PBAT/A40/J0.3; (B) PBAT/A40/10Silk/J0.3; (C) PBAT/A40/J0.5; and (D) PBAT/A40/10Silk/J0.5. The red arrow indicates the fibrils, whereas the red circle indicates the silk powder agglomerates.

could improve the compatibility of PBAT and PLA, the dispersed state of the silk powder and interfacial properties between the silk powder and PBAT/PLA matrix have not improved. As shown in Figure 5, the amounts of fibril formed in the PBAT/PLA matrix are more prevalent but large and smooth silk powder aggregates still exist in the ternary blends even when 0.5 phr Joncryl is added.

Crystallization Properties. Because the crystallization of the polymer matrix could affect the ultimate mechanical properties of the blends, the original crystallinity of the molded specimens was calculated from the curve of the first heating cycle (as shown in Figure 6). PLA in all of the blends showed a cold crystallization temperature of ∼90 °C and melting temperature at ∼168 °C. Although the crystallinity increased with the increasing silk powder contents, the PLA crystallinity in all blends was still lower than pure PLA, compatibilized or not. The enhanced crystallinity of PBAT/PLA composites with increasing silk powder may be caused by the anisotropic nucleation effect of the silk powder in PLA crystallizations, similar to the research completed on other fillers.[30] In the case of our ternary blends, the highest crystallinity of PLA is 19.2% [80(PBAT/A40)/20Silk] but the actual value is only 6% for the composites, when taking the PLA weight percentage into consideration. A very low crystallinity of PLA in the blends hardly accounts for the remarkable dependence of impact toughness on the ternary blends. Except for the first heating, the following cooling and second heating differential scanning calorimetry (DSC) curves are shown in Figure 7. Pure PLA displayed a broad crystallization peak located at 93 °C, whereas pure PBAT shows a sharp crystallization peak at ∼46 °C when cooling at 5 °C/min. When PLA and PBAT were blended together, a sharp crystallization peak appeared at ∼78 °C. We suggest that the blend crystallization peak belongs to the formation of crystals of PLA and PBAT together during the cooling process. The cold crystallization and melting peaks of PLA in the blends are depicted in the second heating curves in Figure 7b,d and both are not influenced by PBAT or silk powder. This means that the crystal structure of PLA is hardly influenced by PBAT and silk in our studies.

Structure and Rheological Analysis. The melt rheology properties are closely related to chain architecture,[31] phase morphology,[32] and interfacial actions.[33] It is important to study the microstructure−process relationship to help understand both the microstructure and thermal process properties of the polymer. The changes in the elastic modulus G', loss modulus G'', and viscosity of the blends without the compatibilizer are shown in Figure 8.

Compared to neat PLA, PBAT shows higher modulus and viscosity because of greater chain entanglement. Therefore, the storage modulus, loss modulus, and viscosity of the matrix for PBAT60/PLA40 were located in the range between that of the pure PBAT and PLA. It was clearly observed that G', G'', and melt viscosity increased with increasing silk powder contents over the entire frequency range. This was due to the poor thermal processability of the silk powder. The silk powder possessed a higher melt flow temperature than its thermal decomposition temperature, which greatly limited its processability during blending. Therefore, it behaved like a reinforcing filler in the melt state, resulting in increased melt modulus and viscosity.

The effect of compatibilizer, Joncryl, on G', G'', and viscosity of the blends is shown in Figure 9. The storage modulus and viscosity of PBAT/PLA/Joncryl are displayed in Figure 9a,c. The incorporation of Joncryl led to increased moduli and

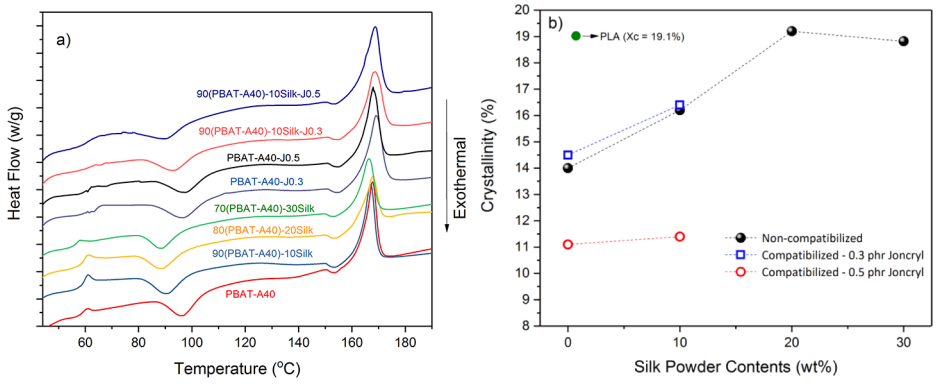

Figure 6. First heating DSC curves of the composites (a) and the corresponding crystallinity calculated from the thermograms of the DSC curves (b)

DOI: 10.1021/acsomega.8b00823
ACS Omega 2018, 3, 12412−12421

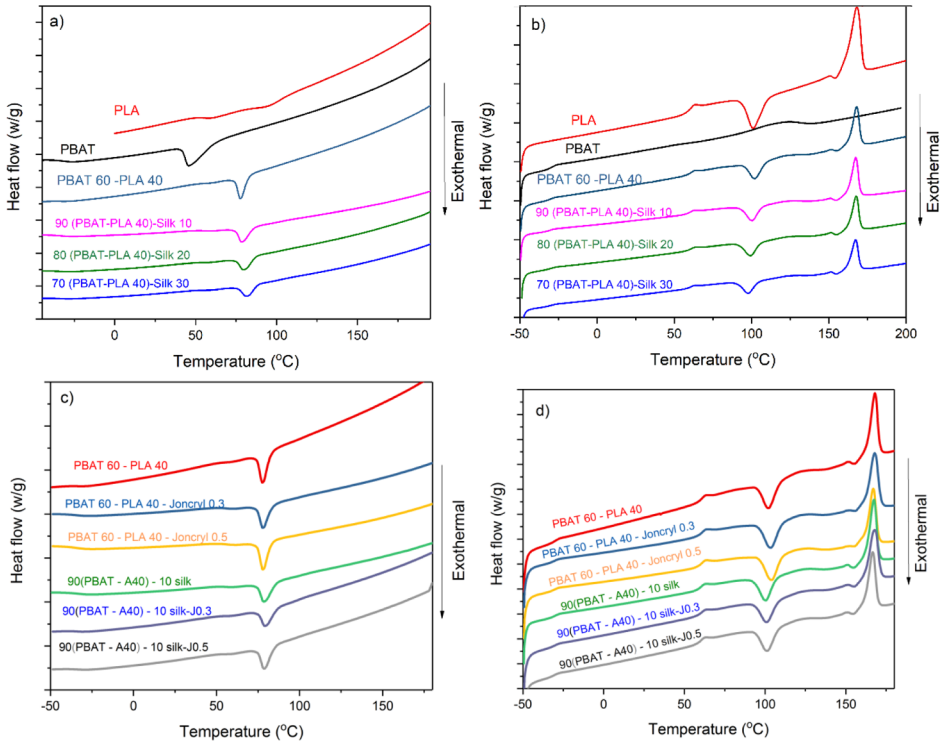

Figure 7. Cooling and second heating DSC curves of the silk powder/polyester blends: (a) noncompatibilized blends cooling at 5 °C/min; (b) noncompatibilized blends heating at 10 °C/min; (c) compatibilized blends cooling at 5 °C/min; and (d) compatibilized blends heating at 10 °C/min.

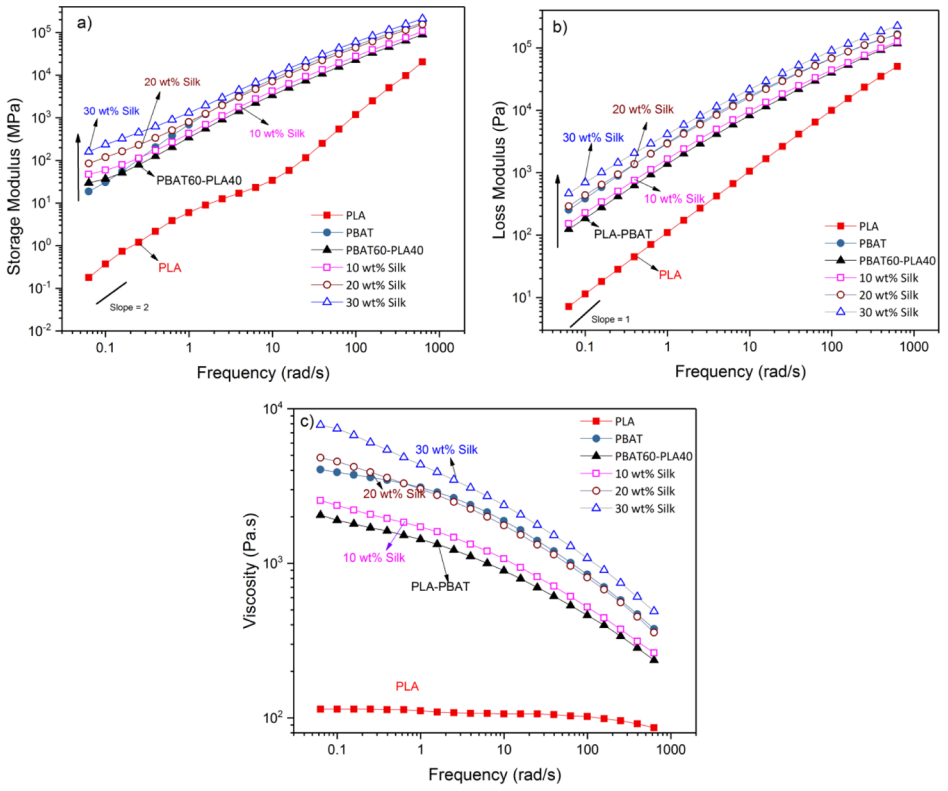

Figure 8. Effect of silk powder loadings on the rheological properties of the blends: (a) storage modulus; (b) loss modulus; and (c) complex viscosity

viscosity for PBAT/PLA blends, especially with 0.5 phr Joncryl. This could be attributed to the possible formation of a PLA/PBAT copolymer in the presence of Joncryl by a reaction during the melt blending process, as indicated in Figure 10. The same behavior was also reported in the previous research.[26,34] However, unlike the PBAT/PLA/Joncryl blends, our PBAT/PLA/silk powder/Joncryl composites showed entirely different rheological properties at 180 °C. The effect of Joncryl on the storage modulus and viscosity of PBAT/PLA/silk ternary blends is depicted in Figure 9b,c, respectively. It is interesting to find

DOI: 10.1021/acsomega.8b00823
ACS Omega 2018, 3, 12412−12421

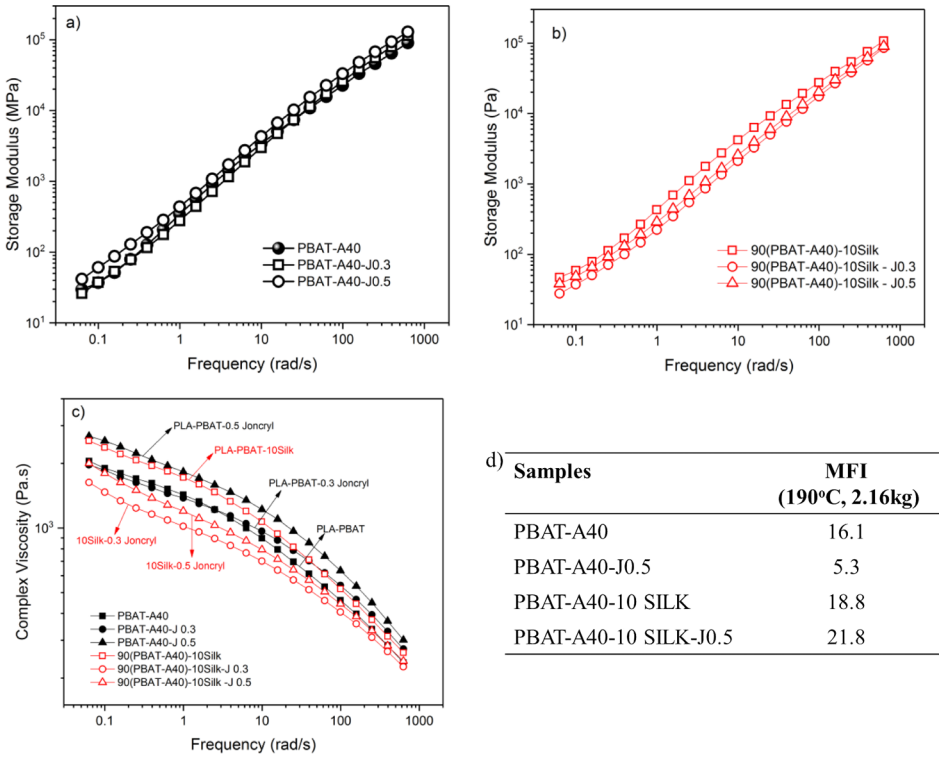

d)

Samples	MFI (190°C, 2.16kg)
PBAT-A40	16.1
PBAT-A40-J0.5	5.3
PBAT-A40-10 SILK	18.8
PBAT-A40-10 SILK-J0.5	21.8

Figure 9. Effect of Joncryl on the rheological properties of the binary and ternary blends: (a) storage modulus; (b) loss modulus; (c) complex viscosity; and (d) MFI values of the representative samples

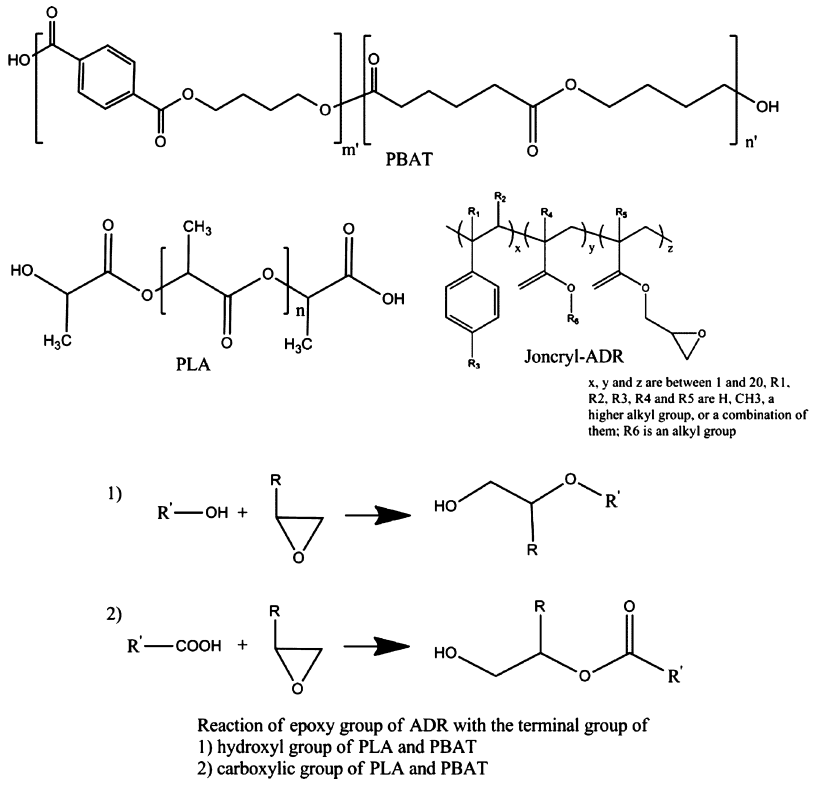

Figure 10. Chemical structure of PLA, PBAT, and Joncryl-ADR and schematic reaction between them during reactive extrusion.

that the storage modulus and viscosity decreased with the addition of Joncryl. An investigation on the structure of silk fibroin by Marsh et al.[35] demonstrated that the chains were tightly packed together by lateral hydrogen bonds, which may cause the poor melt processability. In our case, except for the compatibilizer effect on PLA and PBAT, Joncryl may have also interacted with silk powder to destroy the hydrogen bond of the silk chains, leading to the increased flowability of the silk

DOI: 10.1021/acsomega.8b00823
ACS Omega 2018, 3, 12412−12421

powder. With 0.3 phr Joncryl, the modulus and viscosity of PBAT/PLA/Joncryl blends showed no difference to those of blends without Joncryl, meaning that the compatibilizer effect was limited with low Joncryl content. With 10 wt % silk powder, the weaker hydrogen bonding resulted from the presence of Joncryl, which led to the lowest modulus and viscosity. The modulus and viscosity in the presence of 0.5 phr Joncryl increased slightly because of the competition between the compatibilization and weaker hydrogen bonding effect. The weaker hydrogen bonding caused by Joncryl could benefit the melt processing of this natural polymer, such as the increased melt flow index (MFI) values of the final blends (Figure 9d).

CONCLUSIONS

A natural biopolymer, silk powder, was introduced into synthesized polymer blends of PBAT/PLA by a melt blending method to increase the biocontent of the final material while maintaining the biodegradable properties. A common compatibilizer used with PLA and PBAT blends is Joncryl. Joncryl was added into the PBAT/PLA/silk powder blends to conduct a compatibilization evaluation. The large difference in the polar properties between the natural silk powder and biomaterials PBAT/PLA led to the poor dispersion of silk powder in the blends. The addition of silk powder into PBAT/PLA blends disrupted the integrity of the matrix and no linkage was established at the interface; consequently, the mechanical properties of the blends declined greatly with increasing silk powder content. However, the blends with 10 wt % silk powder still exhibited high notched impact strength of 108 J/m, which indicated the possible applications with high impact properties for the ternary blends. The introduction of the compatibilizer may have increased the performance of PBAT/PLA blends because of the possible esterification reaction which took place within the biopolymer. The increased melt storage modulus and viscosity confirmed the compatibilization effect. However, it was found that Joncryl weakened the hydrogen bonds between the silk chains instead of inducing the compatibilization effect. This is possibly a result of a reaction with the epoxy groups on Joncryl with the polymer. The resulting decreased complex viscosity of the ternary blends with the incorporation of Joncryl indicated that this reaction could be used in the future to improve the processability and dispersion of this natural polymer.

EXPERIMENTAL SECTION

Materials. PLA was supplied by NatureWorks Co., Ltd. with the brand name of Ingeo Biopolymer 3251D with a reported MFI of 35 g/10 min (190 °C/2.16 kg) and relative viscosity of 2.5. PBAT (EcoFlex, film grade) used in this study was obtained from BASF Industry Co., Ltd. This polymer is developed for film extrusion, and blown films with reported MFI between 2.7 and 4.9 g/10 min (190 °C/2.16 kg). Joncryl (ADR-4368, epoxy functional oligomeric acrylic resins) were also purchased from BASF and used as a compatibilizer. The structure of Joncryl was depicted in Figure 10 based on the information provided by the BASF company.[36] The water-soluble superfine silk powder with the size of ∼7 μm was provided by KB Seiren, Ltd. The morphology of the silk powder was observed by SEM and shown in Figure 2. The mean size of the silk powder is around 7 μm, similar to the value provided by the manufacturer. PLA and PBAT pellets as well as silk powder were dried in an oven at 80 °C for 24 h before melt blending.

Biocomposite Fabrication. To prepare the PBAT/PLA/silk powder blends, a masterbatch of PBAT/A40 was first prepared by twin-screw extrusion (Micro-27, Manufactured by Leistritz Corporation, US) at 180 °C, 100 rpm, followed by blending the masterbatch with different amounts of silk powder in a microextrusion/injection molding machine (manufactured by DSM Research, Netherlands) into ASTM standard specimens at melt temperature of 190 °C and mold temperature of 30 °C. The injection processing was conducted at filling pressure of 6 bar, packing pressure of 8 bar, and holding pressure of 8 bar in total 20 s. The masterbatch samples were also prepared in the DSM in same way to make sure that all of the samples experience the same thermal history. The blend formulations and code are shown in Table 2. All test specimens were conditioned for 2 days at 23 °C and 50% relative humidity prior to testing and characterization

Table 2. Compositions of the Reactive Blends and Codes for All of the Specimens

sample	PLA (wt %)	PBAT (wt %)	Silk powder (wt %)	Joncryl (phr)
PLA	100	0	0	0
PBAT	0	100	0	0
PBAT/A40	40	60	0	0
PBAT/A40/J0.3				0.3
PBAT/A40/J0.5				0.5
90(PBAT/A40)/10Silk	36	54	10	0
90(PBAT/A40)/10Silk/J0.3				0.3
90(PBAT/A40)/10Silk/J0.5				0.5
80(PBAT/A40)/20Silk	32	48	20	0
70(PBAT/A40)/30Silk	28	42	30	0

Characterization Methods. *Mechanical Property Tests.* The tensile and flexural properties of the samples were tested on an Instron mechanical testing (Instron 3382 equipped with an extensometer, manufactured by Instron, US) system according to the ASTM standards D638 and D790, respectively. Izod impact testing of notched samples was carried out as per ASTM D256 by a Testing Machine Inc. (TMI) instrument (Testing Machine Inc. US). In all mechanical tests, the reported data are the mean and standard deviation. At least five specimens are tested for each sample.

Rheology Tests. The rheological behaviors of the composites were studied using a rheometer (Anton-Paar MCR-302 Instrument). The frequency-dependent rheology behavior of all of the samples was monitored at 180 °C, 1% strain under N_2 protection. The testing samples were injected as a disk (diameter: 25 mm, thickness: 1 mm) shape at 180 °C using a micro 15 cm^3 corotating twin screw compounder and micro 12 cm^3 DSM injection molding machine (manufactured by DSM Research, Netherlands).

Differential Scanning Calorimetry. DSC measurements were performed on a TA Q200 DSC instrument under a N_2 atmosphere. First, the samples were heated to 220 °C with a heating rate of 10 °C/min and maintained at that temperature for 3 min before cooling to −70 °C at a rate of 10 °C/min. After that the second heating scans were monitored between −70 and 220 °C at a heating rate of 10 °C/min for determining the glass-transition temperature (T_g), cold crystallization temperature (T_{cc}), melting temperature (T_m), and crystallinity (X_c).

The crystallinity of PLA (X_{PLA}) was calculated based on the melting enthalpy (ΔH_{PLA}) at ∼167 °C, cold crystallization

DOI: 10.1021/acsomega.8b00823
ACS Omega 2018, 3, 12412−12421

enthalpy of PLA (ΔH_{cPLA}), and the weight ratio of PLA (W_{PLA}), as illustrated in eq 1.

$$X_c = \frac{\Delta H'_m - \Delta H_c}{w'_f \Delta H^o_m} \times 100\% \quad (1)$$

where $\Delta H'_m$ and ΔH_c are the melting enthalpies and cold crystallization enthalpies of PLA, respectively, ΔH^o_m is the melting assuming 100% crystalline PLA (93.7 J/g),[37] and w'_f is the weight fraction of PLA in the blend.

Scanning Electron Microscopy. The morphology of the blends was observed by Hitachi S-570 SEM with an accelerating voltage of 10 KV. The fracture surfaces obtained from the notched Izod impact test were sputtered with gold and characterized by SEM directly.

MFI Tests. The MFI was tested on MFI-2000A Melt Flow Indexer according to the ASTM D1238. The test was conducted at 190 °C, 2.16 kg.

AUTHOR INFORMATION

Corresponding Authors

*E-mail: hirai@mmm.muroran-it.ac.jp (S.H.).
*E-mail: mmisra@uoguelph.ca (M.M.).

ORCID

Amar K. Mohanty: 0000-0002-1079-2481
Manjusri Misra: 0000-0003-2179-7699

Notes

The authors declare no competing financial interest.

ACKNOWLEDGMENTS

The authors would like to acknowledge the financial support by the Natural Sciences and Engineering Research Council (NSERC), Canada Discovery Grants Project # 400320 and 401111; the Ontario Research Fund, Ontario Research Fund, Research Excellence Program, Round-7 (ORF-RE07) from the Ontario Ministry of Research and Innovation, currently known as the Ontario Ministry of Research, Innovation and Science (MRIS) project # 052644 and 052665; and the Ontario Ministry of Agriculture, Food and Rural Affairs (OMAFRA)/University of Guelph Gryphon's LAAIR Program (project # 298635).

REFERENCES

(1) Reddy, M. M.; Vivekanandhan, S.; Misra, M.; Bhatia, S. K.; Mohanty, A. K. Biobased plastics and bionanocomposites: Current status and future opportunities. *Prog. Polym. Sci.* **2013**, *38*, 1653−1689.
(2) Sionkowska, A. Current research on the blends of natural and synthetic polymers as new biomaterials: Review. *Prog. Polym. Sci.* **2011**, *36*, 1254−1276.
(3) Bastioli, C.; Bellotti, V.; Giudice, L.; Gilli, G. Mater-Bi: Properties and biodegradability. *J. Environ. Polym. Degrad.* **1993**, *1*, 181−191.
(4) Wang, Y.; Kim, H.-J.; Vunjak-Novakovic, G.; Kaplan, D. L. Stem cell-based tissue engineering with silk biomaterials. *Biomaterials* **2006**, *27*, 6064−6082.
(5) Fini, M.; Motta, A.; Torricelli, P.; Giavaresi, G.; Nicoli Aldini, N.; Tschon, M.; Giardino, R.; Migliaresi, C. The healing of confined critical size cancellous defects in the presence of silk fibroin hydrogel. *Biomaterials* **2005**, *26*, 3527−3536.
(6) Tamada, Y. New process to form a silk fibroin porous 3-D structure. *Biomacromolecules* **2005**, *6*, 3100−3106.
(7) Wang, X.; Hu, X.; Daley, A.; Rabotyagova, O.; Cebe, P.; Kaplan, D. L. Nanolayer biomaterial coatings of silk fibroin for controlled release. *J. Controlled Release* **2007**, *121*, 190−199.
(8) Takeshita, H.; Ishida, K.; Kamiishi, Y.; Yoshii, F.; Kume, T. Production of fine powder from silk by radiation. *Macromol. Mater. Eng.* **2000**, *283*, 126−131.
(9) Rajkhowa, R.; Wang, L.; Wang, X. Ultra-fine silk powder preparation through rotary and ball milling. *Powder Technol.* **2008**, *185*, 87−95.
(10) Kaneko, A.; Tamada, Y.; Hirai, S.; Kuzuya, T.; Hashimoto, T. Characterization of a Silk-Resinified Compact Fabricated Using a Pulse-Energizing Sintering Device. *Macromol. Mater. Eng.* **2012**, *297*, 272−278.
(11) Chen, H.; Hu, X.; Cebe, P. Thermal properties and phase transitions in blends of Nylon-6 with silk fibroin. *J. Therm. Anal. Calorim.* **2008**, *93*, 201−206.
(12) Tanaka, T.; Tanigami, T.; Yamaura, K. Phase separation structure in poly(vinyl alcohol)/silk fibroin blend films. *Polym. Int.* **1998**, *45*, 175−184.
(13) Liu, H.; Xu, W.; Zou, H.; Ke, G.; Li, W.; Ouyang, C. Feasibility of wet spinning of silk-inspired polyurethane elastic biofiber. *Mater. Lett.* **2008**, *62*, 1949−1952.
(14) Gao, Q.; Shao, Z.; Sun, Y.; Lin, H.; Zhou, P.; Yu, T. Complex Formation of Silk Fibroin with Poly(acrylic acid). *Polym. J.* **2000**, *32*, 269−274.
(15) Xu, W.; Wang, X.; Li, W.; Peng, X.; Liu, X.; Wang, X. G. Characterization of Superfine Wool Powder/Poly(propylene) Blend Film. *Macromol. Mater. Eng.* **2007**, *292*, 674−680.
(16) Dang, J.; Leong, K. Natural polymers for gene delivery and tissue engineering. *Adv. Drug Delivery Rev.* **2006**, *58*, 487−499.
(17) Rho, K. S.; Jeong, L.; Lee, G.; Seo, B.-M.; Park, Y. J.; Hong, S.-D.; Roh, S.; Cho, J. J.; Park, W. H.; Min, B.-M. Electrospinning of collagen nanofibers: effects on the behavior of normal human keratinocytes and early-stage wound healing. *Biomaterials* **2006**, *27*, 1452−1461.
(18) Cascone, M. G.; Sim, B.; Sandra, D. Blends of synthetic and natural polymers as drug delivery systems for growth hormone. *Biomaterials* **1995**, *16*, 569−574.
(19) Arvanitoyannis, I. S. Totally and Partially Biodegradable Polymer Blends Based on Natural and Synthetic Macromolecules: Preparation, Physical Properties, and Potential as Food Packaging Materials. *J. Macromol. Sci., Part C: Polym. Rev.* **1999**, *39*, 205−271.
(20) Vieira, M. G. A.; da Silva, M. A.; dos Santos, L. O.; Beppu, M. M. Natural-based plasticizers and biopolymer films: A review. *Eur. Polym. J.* **2011**, *47*, 254−263.
(21) Nagarajan, V.; Mohanty, A. K.; Misra, M. Perspective on Polylactic Acid (PLA) based Sustainable Materials for Durable Applications: Focus on Toughness and Heat Resistance. *ACS Sustainable Chem. Eng.* **2016**, *4*, 2899−2916.
(22) Mohanty, S.; Nayak, S. K. Biodegradable Nanocomposites of Poly(butylene adipate-co-terephthalate) (PBAT) and Organically Modified Layered Silicates. *J. Polym. Environ.* **2012**, *20*, 195−207.
(23) Fukushima, K.; Wu, M.-H.; Bocchini, S.; Rasyida, A.; Yang, M.-C. PBAT based nanocomposites for medical and industrial applications. *Mater. Sci. Eng., C* **2012**, *32*, 1331−1351.
(24) Miles, I. S.; Zurek, A. Preparation, structure, and properties of two-phase co-continuous polymer blends. *Polym. Eng. Sci.* **1988**, *28*, 796−805.
(25) Farsetti, S.; Cioni, B.; Lazzeri, A. Physico-Mechanical Properties of Biodegradable Rubber Toughened Polymers. *Macromol. Symp.* **2011**, *301*, 82−89.
(26) Al-Itry, R.; Lamnawar, K.; Maazouz, A. Improvement of thermal stability, rheological and mechanical properties of PLA, PBAT and their blends by reactive extrusion with functionalized epoxy. *Polym. Degrad. Stab.* **2012**, *97*, 1898−1914.
(27) Ma, P.; Cai, X.; Zhang, Y.; Wang, S.; Dong, W.; Chen, M.; Lemstra, P. J. In-situ compatibilization of poly(lactic acid) and poly(butylene adipate-co-terephthalate) blends by using dicumyl peroxide as a free-radical initiator. *Polym. Degrad. Stab.* **2014**, *102*, 145−151.
(28) Abdelwahab, M. A.; Taylor, S.; Misra, M.; Mohanty, A. K. Thermo-mechanical characterization of bioblends from polylactide and poly(butylene adipate-co-terephthalate) and lignin. *Macromol. Mater. Eng.* **2015**, *300*, 299−311.
(29) Liu, H.; Song, W.; Chen, F.; Guo, L.; Zhang, J. Interaction of Microstructure and Interfacial Adhesion on Impact Performance of

DOI: 10.1021/acsomega.8b00823
ACS Omega 2018, 3, 12412−12421

Polylactide (PLA) Ternary Blends. *Macromolecules* **2011**, *44*, 1513−1522.
(30) Liao, R.; Yang, B.; Yu, W.; Zhou, C. Isothermal cold crystallization kinetics of polylactide/nucleating agents. *J. Appl. Polym. Sci.* **2007**, *104*, 310−317.
(31) Dorgan, J. R.; Williams, J. S.; Lewis, D. N. Melt rheology of poly(lactic acid): Entanglement and chain architecture effects. *J. Rheol.* **1999**, *43*, 1141−1155.
(32) Wu, S. Formation of dispersed phase in incompatible polymer blends: Interfacial and rheological effects. *Polym. Eng. Sci.* **1987**, *27*, 335−343.
(33) Wu, F.; Zhang, S.; Chen, Z.; Zhang, B.; Yang, W.; Liu, Z.; Yang, M. Interfacial relaxation mechanisms in polymer nanocomposites through the rheological study on polymer/grafted nanoparticles. *Polymer* **2016**, *90*, 264−275.
(34) Al-Itry, R.; Lamnawar, K.; Maazouz, A. Reactive extrusion of PLA, PBAT with a multi-functional epoxide: Physico-chemical and rheological properties. *Eur. Polym. J.* **2014**, *58*, 90−102.
(35) Marsh, R. E.; Corey, R. B.; Pauling, L. An investigation of the structure of silk fibroin. *Biochim. Biophys. Acta* **1955**, *16*, 1−34.
(36) https://www.basf.com/us/en/products-and-industries/General-Business-Topics/dispersions/Products/joncryl0.html.
(37) Wu, F.; Zhang, S.; Zhang, B.; Yang, W.; Liu, Z.; Yang, M. The effect of the grafted chains on the crystallization of PLLA/PLLA-grafted SiO2 nanocomposites. *Colloid Polym. Sci.* **2016**, *294*, 801−813.

DOI: 10.1021/acsomega.8b00823
ACS Omega 2018, 3, 12412−12421